

Preparation and optimization of nanoporous hollow carbon spheres /S composite cathode materials for Li-S battery

Wenhua Zhang^{1,3}, Ping Liu², Jiabin Pan⁴, Xiaopin Yang^{1,3}, Jia Liu^{1,3}, Huijun Xu^{1,3}, Zhizhao Ouyang^{1,3}

¹ Nanchang Institute of Technology, Tianxiang Avenue No.289, 330099, Nanchang, China

² State Grid Jiangxi Electric Power Company Limited research institute, Minqiang Road No.88, 330096, Nanchang, China

³ Nanchang Institute of Technology, Jiangxi Province Key Laboratory of Precision Drive and Control, Tianxiang Avenue No.289, 330099, Nanchang, China

⁴ Guangxi science and technology intelligence institute, Xinghu road No.24, 530022 Nanning, China

*E-mail: zhangwenhua_610@163.com

Received: 2 January 2019 / Accepted: 14 March 2019 / Published: 10 April 2019

Aiming at the problems of dissolution and volume expansion of intermediates in lithium-sulfur batteries during the reaction process, a high-porosity mesoporous carbon sphere with hollow structure (labeled as PS-hollow carbon) is prepared by polystyrene(PS) template method. As a conductive matrix for sulfur electrode, it not only increases the sulfur load, but also adsorbs the polysulfide in the hollow structure of the sphere and the mesoporous pores of the shell. And with the β -Cyclodextrin as the sticking agent, the polysulfide ions are bound to the interior of hollow carbon by surface enveloping, which inhibits the dissolution of active materials. Scanning electron microscopy (SEM), transmission electron microscopy (TEM), and nitrogen adsorption and desorption characterization indicated that porous carbon has a hollow spherical structure with mesoporous pores (pore diameter of 2~4nm on the surface). The X-ray diffraction (XRD) pattern indicates that the elemental sulfur is uniformly dispersed in the hollow carbon pore structure. The thermogravimetric analysis showed that the sulfur content of PS-hollow carbon/S composite is 74.8 wt.%. The electrochemical test showed that the as-prepared carbon/sulfur composite can deliver a reversible capacity of 1445 mAh g⁻¹ at the first cycle, and remained above 750 mAh g⁻¹ after 100 cycles, indicating that the PS-carbonized carbon/S composite has good electrochemical activity and cycle stability.

Keywords: High Pore Volume; Hollow Carbon Sphere; Carbon/Sulfur Composites; Li-S Battery

1. INTRODUCTION

The ever-increasing demand for electric energy storage, ranging from portable electronics to electric vehicles and to renewable power stations, stimulates the development of improved rechargeable

lithium batteries with substantially enhanced energy density and greatly reduced cost[1,2]. In this technology development, lithium-sulfur batteries (Li-S) are revisited as a promising candidate for large scale electric storage, because of its high theoretical energy density of 2600 Wh Kg^{-1} and particularly the natural abundance and low toxicity of sulfur, which has great development and application prospects[3-5]. Despite a great progress has been achieved, commercial development of Li-S batteries is still hindered by the insufficient cyclability and low utilization of the electrode-active materials, which are given rise by the insulating nature of sulfur and its discharge products (Li_2S_2 and Li_2S), the dissolution loss of the intermediates generated during discharge of sulfur, and the volume expansion from sulfur to Li_2S [6].

In order to address the above problems, considerable efforts have been made in the past decade. One of the major strategies is to impregnate sulfur into the nanopores of conductive carbon matrix, aiming to make the sulfur electrode electrically active and trap soluble polysulphides in the nanopores avoiding the loss of active material. Various nanostructured carbon materials, such as including carbon nanotubes[7,8], carbon nanofibers[9-11], microporous carbon[12,13], mesoporous carbon[14,15], porous hollow carbon spheres[16,18], carbon nanospheres[19,20], graphene[21-23], etc, which have been widely used as sulfur carriers due to their excellent electrical conductivity and large specific surface area, abundant pore structure, which provide not only an electrochemical reaction framework with high conductivity and structural stability for sulfur and lithium sulfide, but also can inhibit the diffusion of soluble polysulfide ions to the electrolyte.

Meanwhile, different morphology and pore structure of carbon carrier lead to different performance of the sulfur electrode. For example, mesoporous carbon has large specific surface area and pore volume, controllable pore diameter distribution and ordered pore structure, particularly, carbon nanotubes and CMK-3[14,24]. As sulfur carrier, the interconnected mesoporous pipeline not only facilitates the transmission of solvated Li^+ during charging and discharging, but also help to trap the dissolved polysulfide anions within the porous. CMK-3/S composites with 70% sulfur load showed a reversible capacity of over 1000 mA h g^{-1} after 20 cycles. However, the cycle performance remains an issue for this kind of sulfur cathodes. It is possible that mesoporous dsorption capacity is limited for polysulphide.

With the development of research, microporous carbon was found to have an particular limiting effect and strong adsorption on sulfur and soluble polysulfide ions, and shows different charging and discharging phenomena from conventional lithium sulfur batteries and better electrochemical properties, because the active material exit in form of chain-like small molecule sulfur S_{2-4} in small size pores ($< 0.7\text{nm}$)[13,25]. However, there are also two obvious disadvantages: (1) due to the limited pore capacity of microporous carbon, the sulfur content of microporous carbon as a sulfur carrier is generally difficult to exceed 50%. (2) the discharge platform of microporous carbon/sulfur composite anode materials is relatively low, which limits the improvement of energy density of li-sulfur batteries.

Based on the above analysis, microporous carbon has an effective limiting effect and strong adsorption on sulfur and soluble polysulfide ions. Mesopores promote the flow of electrolyte and the transport of lithium ions, while macropores can further improve the ionic conductivity and sulfur load. As such, development of novel multilevel porous carbon used as sulfur host is highly desirable. Jung [26] synthesized a multistage structure porous carbon particle. Meso-pores and macro-pores in the

porous carbon are surrounded by a large number of micro-pores, forming a nearly closed structure. Jayaprakash[16] used a hollow carbon sphere with mesoporous shell structure as sulfur carrier. The assembled Li-S batteries exhibit good electrochemical properties, while the sulfur loading is unable to satisfy the industrial development of the Li-S battery.

In addition, since the density of Li_2S (1.67 g cm^{-3}) is lower than that of S (2.03 g cm^{-3}), the carbon matrix needs to withstand the mechanical stress caused by the volume expansion of sulfur during the charge-discharge process. It is reported that 22% volume change is accompanied during the charge-discharging cycle of the sulfur electrode[27]. And then, a high porosity mesoporous carbon sphere with hollow structure was prepared in our work, The sulfur/carbon composite material with high sulfur content (~75%) was obtained by partly filling the sulfur into the mesoporous pores of the hollow structure and shell through heat treatment. Furthermore, the electrochemical properties of the composite sulfur electrode were investigated and improved.

2. EXPERIMENT

2.1 Material preparation

2.1.1 Preparation of PS Template

140 mL of distilled water, 17.5 mL of styrene and 1.44 mL of acrylic acid are added into a 250 mL flask. The mixture is stirred well in an 80°C oil bath pot. 0.15g potassium persulfate dissolved in 10 mL distilled water is added to the above solution drop by drop, and the reaction lasts 8 hours. The product solution is collected by spray drying and the PS template has been prepared[28].

2.1.2 Preparation of PS- hollow Carbon

2g PS template prepared and 5g 20 wt.% phenolic resin are added into 100 mL flask. The mixture is sonicated for 10 min and stirred for 30 min. After steaming at 50°C and drying, the solid product is pyrolyzed for 2 h at 900°C with a heating rate of $5^\circ \text{C} / \text{min}$ in Ar atmosphere. Then, high-porosity hollow carbon (labeled PS-hollow carbon) is prepared by activation in CO_2 for 1 hour. The product is labeled as PS-hollow carbon.

2.1.3 Preparation of PS- hollow Carbon /S Composites

PS-hollow carbon /S composites are prepared by gas phase adsorption. The specific operation process is as follows: Sufficient elemental sulfur and a certain amount of mesoporous carbon were placed in two sample bottles respectively, which are put in sealed jar filled with Ar gas. After 400°C heating for 5 hours, sulfur steam is absorbed into the mesoporous carbon pores, and the hollow carbon/S composite material achieved. The thermogravimetric analysis showed that the sulfur content of PS-hollow carbon/S composite is 74.8 wt.%

2.2 Representation

The structure of elemental sulfur and high-porosity carbon materials and the distribution of elemental sulfur in carbon matrix pores were characterized by X-ray diffraction instrument (XRD-6000, Shimadzu, Cu K α , Shimadzu corporation of Japan, scanning speed is: 4 ° / min, the scanning range is: 10 ° to 80 °). The surface and internal structure of hollow mesoporous carbon materials were characterized by scanning electron microscope (Quanta 200, Dutch FEI company) and transmission electron microscope (JEOL JEM-2010FEF, Japanese electronics co., LTD). The specific surface area and pore structure parameters of hollow mesoporous carbon materials were characterized by nitrogen adsorption instrument (JW-BK, Beijing subtle grace technology co., LTD.). The sulfur content in sulfur complex was characterized by thermogravimetric analyzer (Q500, TA companies in the United States).

2.3 Electrochemical test

2.3.1 Cell preparation

The composite sulfur electrode is prepared by using PVDF and β -Cyclodextrin as binder. The specific preparation process is as follows: (1) The PS-hollow carbon /S composite material was mixed with acetylene black and PVDF at a mass ratio of 80:10:10 and then stirred for 1-4 hours. (2) The PS-hollow carbon /S composite was mixed with acetylene black and β -Cyclodextrin by a mass ratio of 70:15:15, and then stirred for 1-4 hours. Then, apply the above slurry evenly on the aluminum foil collector fluid with spatula respectively. After vacuum drying at 60 °C, the film is cut into small rounds of about 1 cm in diameter to assembly 2016 type button cell. And the electrolyte is Soluble ether electrolyte (1M LiTFSI/DOL-DME(1:1,v/v)).

2.3.2 The Performance Test

The charge-discharge test of the button battery was conducted by battery charge-discharge instrument (LAND/2001A, Wuhan blue electronic co. LTD.) The cyclic and multiplier properties of the sulfur electrode were investigated, and the test voltage range was 1.7-3.1V. The cyclic voltammetry curve of the battery is tested by electrochemical workstation (Shanghai chenhua instrument co. LTD.).

3. RESULTS AND DISCUSSION

3.1 Structure Analysis

Fig. 1 shows the SEM photo (a) and TEM photo (b) of hollow carbon prepared by PS template. As shown in fig. 1(a), PS-hollow carbon prepared by PS template is uniform spherical with a diameter of about 300 nm~400 nm. Some of the spheres are glued together by the carbon layer on the surface. It can be seen from fig. 1(b) that the PS-hollow carbon has a clear hollow ball structure, with adhesion

between the spheres, corresponding to the SEM photographs. The carbon shell is about 50 nm thick with porous structure.

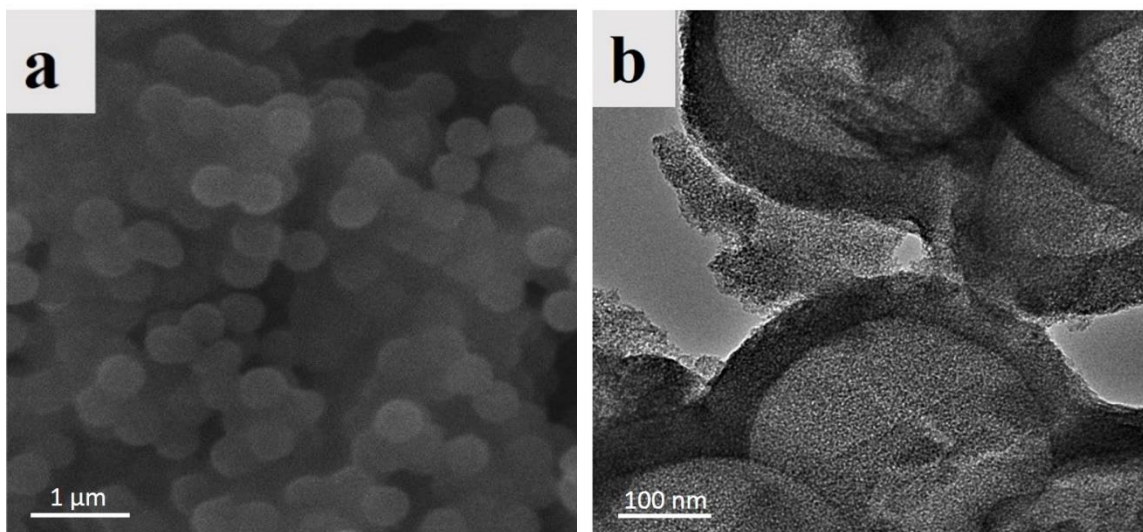


Figure 1. SEM photo(a) and TEM photo(b) of PS-hollow carbon

The isothermal adsorption curve and pore size distribution of PS-hollow carbon are shown in fig. 2. As shown in fig. 2(a), the isotherm of hollow carbon belongs to type IV in IUPAC classification[29]. The N₂ gas desorption mainly occurs in the regions with relatively low pressure. And the hysteric loop of H3 is presented under relatively high pressure, indicating that the pore structure of PS-hollow carbon activated by CO₂ is mainly mesoporous. As seen in fig. 2(b), hollow carbon has relatively uniform pore size and narrow distribution, and the pore size range is mainly between 2 nm-4 nm. The specific surface area of the activated carbon is 1210 m² g⁻¹, calculated by BET method. The pore volume of the activated carbon is 1.1cm³ g⁻¹ by fitting the adsorption isotherm branches with BJH method, and the pores are mainly mesoporous.

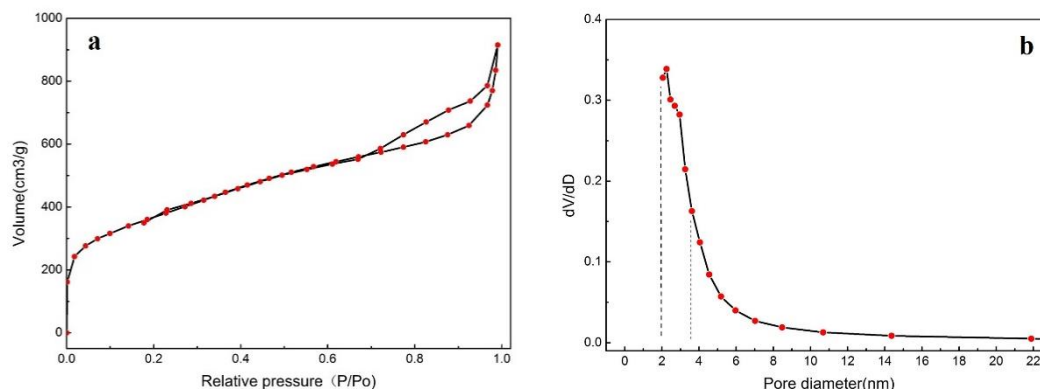


Figure 2. Isothermal adsorption and desorption curve (a) and pore size distribution of PS- hollow carbon (b)

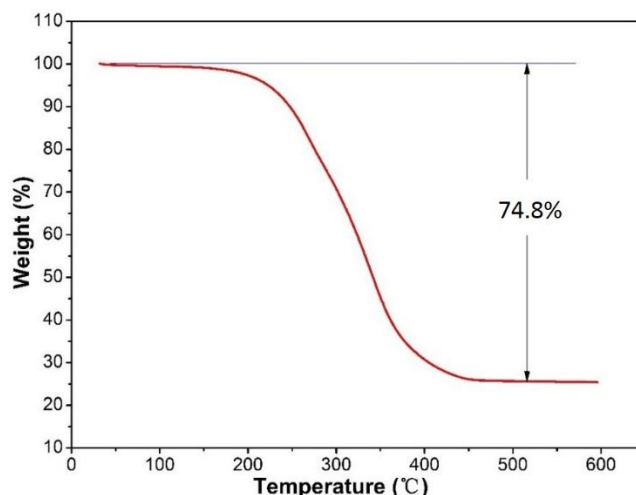


Figure 3. thermogravimetric analysis curve of PS- hollow carbon /S composite

In order to investigate the composite of elemental sulfur in hollow carbon, PS- hollow carbon /S is analyzed and characterized by TG and XRD. Fig. 3 shows the thermogravimetric analysis curve of PS- hollow carbon /S composite. As shown, most of elemental sulfur weightlessness mainly occurs between 200 °C to 400 °C. The weightlessness completely after 500°C, and the whole weight loss percentage is 74.8%. Thus, the sulfur content of PS-hollow carbon /S composite material is 74.8 wt.%, which is consistent with the result of the change of carbon matrix mass before and after the gas phase adsorption of sulfur. Such a high sulfur load is not common in similar sulfur-carbon composites.

Fig. 4 shows the X-ray diffraction pattern before and after the composite of elemental sulfur and PS-hollow carbon. Among them, XRD patterns of elemental sulfur show sharp diffraction peaks, indicating that elemental sulfur exists in crystalline form. And PS-hollow carbon presents two broad diffraction packages which located at 2θ of about 24.5° and 44.8° , corresponding to the diffraction peaks of graphite (002) and (101) crystal plane respectively, indicating that the PS-hollow carbon sphere materials have graphite microcrystals and good electrical conductivity [30]. When sulfur is loaded onto the hollow charcoal, the composite exhibits a diffraction envelope only around 24.5° , indicating that elemental sulfur is uniformly dispersed in the pore structure of PS-carbon hollow in an amorphous structure or in the form of tiny nanocrystals[12]. High dispersion of elemental sulfur in hollow carbon matrix can improve the electrochemical activity and cyclic stability of sulfur electrode.

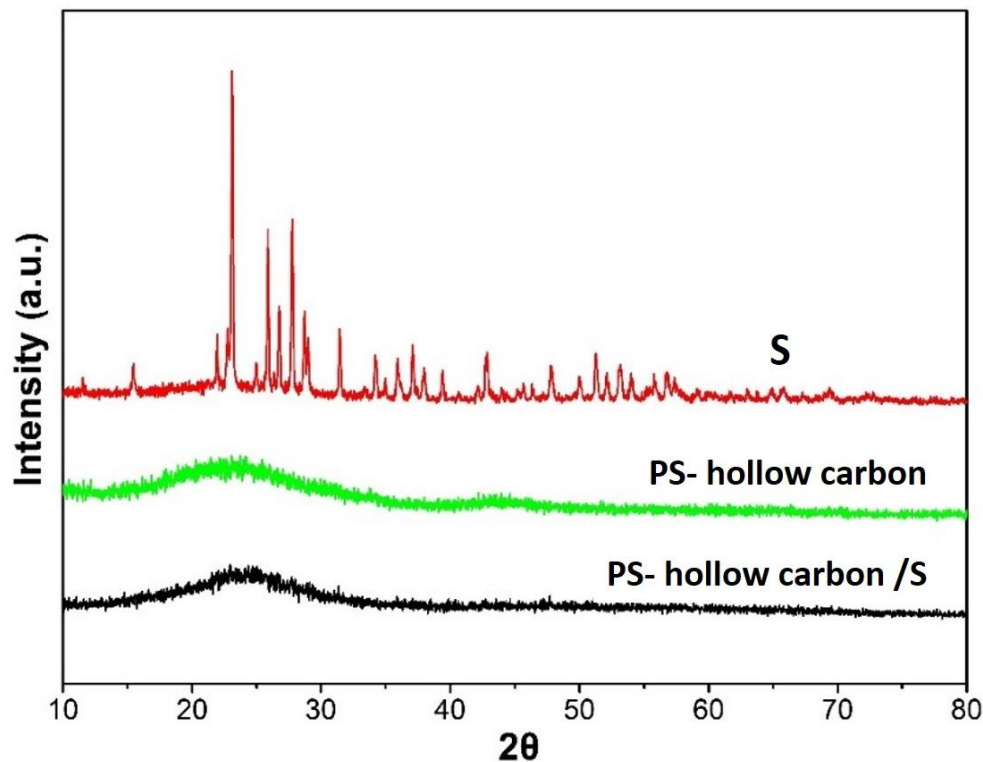


Figure 4. X-ray diffraction patterns of sulfur, PS- hollow carbon and PS- hollow carbon /S composite materials

Fig. 5 shows the cyclic voltammetry curve of PS-hollow carbon/S composite in 1 M LiTFSI/DOL-DME electrolyte. As shown, there are two obvious reduction peaks at 2.2V and 2.0V in the first cycle, corresponding to the transformation from S_8 to polysulfide S_x^{2-} ($x=4-6$) and from polysulfide S_x^{2-} ($x=4-6$) to Li_2S_2 and Li_2S [4]. In addition, a weak broad peak is also observed at 2.5V, which disappeared in the subsequent scanning process and irreversible. It may be the reduction of oxygen groups on the surface of hollow mesoporous carbon or small amount of impurity gas molecules (O_2 and SO_2) remaining in the pore channel [15]. In the subsequent forward scanning process, an obvious oxidation peak and a less obvious acromial peak, respectively at 2.45V and 2.64V, corresponding to the transformation of Li_2S_2 and Li_2S to polysulfide S_x^{2-} ($x=4-6$) and the transformation of polysulfide S_x^{2-} ($x=4-6$) to S_8 [4]. It shows that PS-hollow carbon/S composite has good electrochemical reversibility. The acromial peak at 2.64V is weak and disappeared in the subsequent scanning process, indicating that the conversion rate of the transformation of polysulfide to elemental sulfur is very low and it is a difficult oxidation process [5]. It can also be seen from the figure that the curves of the second and fifth cycles basically coincide. Compared with the first cycle of CV curves, reduction peaks shift in the direction of the oxidation peak, and oxidation peak shift towards reduction peaks, which shown electrochemical polarization is reduced. This is mainly because in the first cycle of the reaction process, electrolyte infiltration into the composite channel and infiltration of the active material takes some time, so there is a first-cycle voltage lag phenomenon. Starting from the second cycle, lithium ions are easier to migrate to the surface of the active material after the electrolyte infiltrates, thus reducing the polarization during the sulfur electrode reaction process [7].

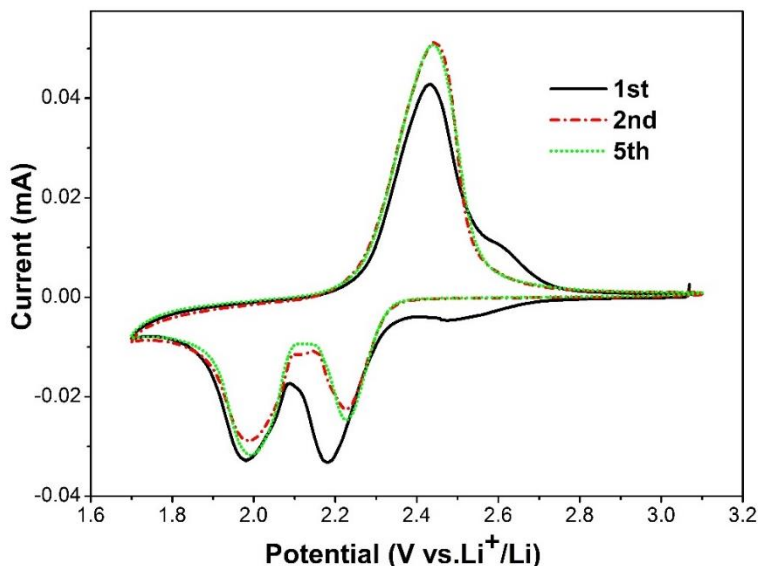


Figure 5. Cyclic voltammetry curve of PS- hollow carbon /S composite in 1 M LiTFSI/ DOL-DME electrolyte, scanning rate: 0.05 mV s^{-1} , voltage range: 1.7 V - 3.1 V

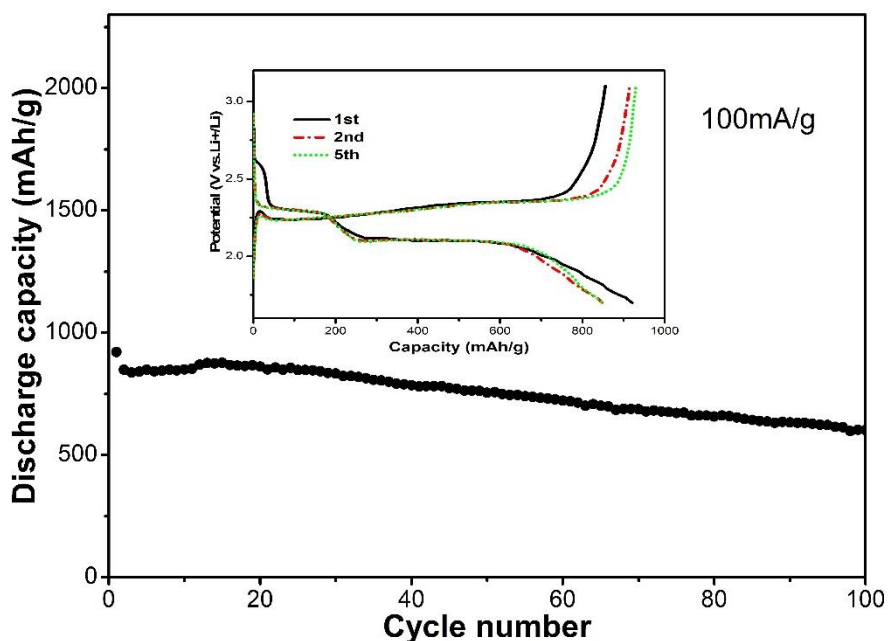


Figure 6. Cycle performance and charge-discharge curve of PS- hollow carbon /S composite in 1 M LiTFSI/ DOL-DME electrolyte, current density: 100 mA g^{-1} , voltage range: 1.7-3.1V

The cycling performance and charge-discharge curve of PS-hollow carbon/S composite electrode in 1 M LiTFSI/ DOL-DME electrolyte is shown in figure 6. As shown, the composite electrode has two discharge platforms at 2.3 V and 2.1 V, respectively, which are assigned to the ringopening of S8 and the reduction of polysulfides to Li_2S_2 and Li_2S . It is consistent with the typical discharge characteristics of sulfur electrode [6]. In the subsequent charging process, the voltage platform is located between 2.25 v-2.35 V. As the cycle goes on, the charging and discharging platform of the electrode are remain stable, indicating that the nanoporous hollow carbon sphere can provide a good conducting network for the

sulfur. In the early 20 cycles of the performance curve in figure 6 (out), there is no attenuation in capacity, but shows a gradual upward trend. That is probably due to the improvement of the infiltration of electrolyte and the increased utilization of active materials[9]. The discharge capacity of the composite sulfur electrode is 920 mAh g^{-1} in the first cycle, and remained above 620 mAh g^{-1} after 100 cycles, with a capacity retention rate of 67.4%, showing a good cycle stability. Compared with PS-hollow carbon/S electrode, the initial discharge of the HNC-S composites in the literature is 1108 mAh g^{-1} and reduced to 558 mAh g^{-1} and 450 mAh g^{-1} after 100 and 150 cycles respectively, with a capacity retention of 50.9% and 40.6% [18]. It is indicated that the PS-hollow carbon with multilevel pore structure prepared facilitates the impregnation of electrolyte, ensures the rapid transfer of lithium ions, and effectively inhibiting the diffusion of polysulfide ions to the electrolyte, thus reducing the shuttle effect. The hollow carbon spheres with structural stability and excellent electrical conductivity provide a good electrochemical reaction site for the active materials and enough space volume expansion during charge and discharge [31].

In order to further improve the electrochemical properties of PS-hollow carbon /S composite materials, the β -Cyclodextrin is selected as a binder. And the performance of composite sulfur electrode prepared by PVDF and β -Cyclodextrin was compared.

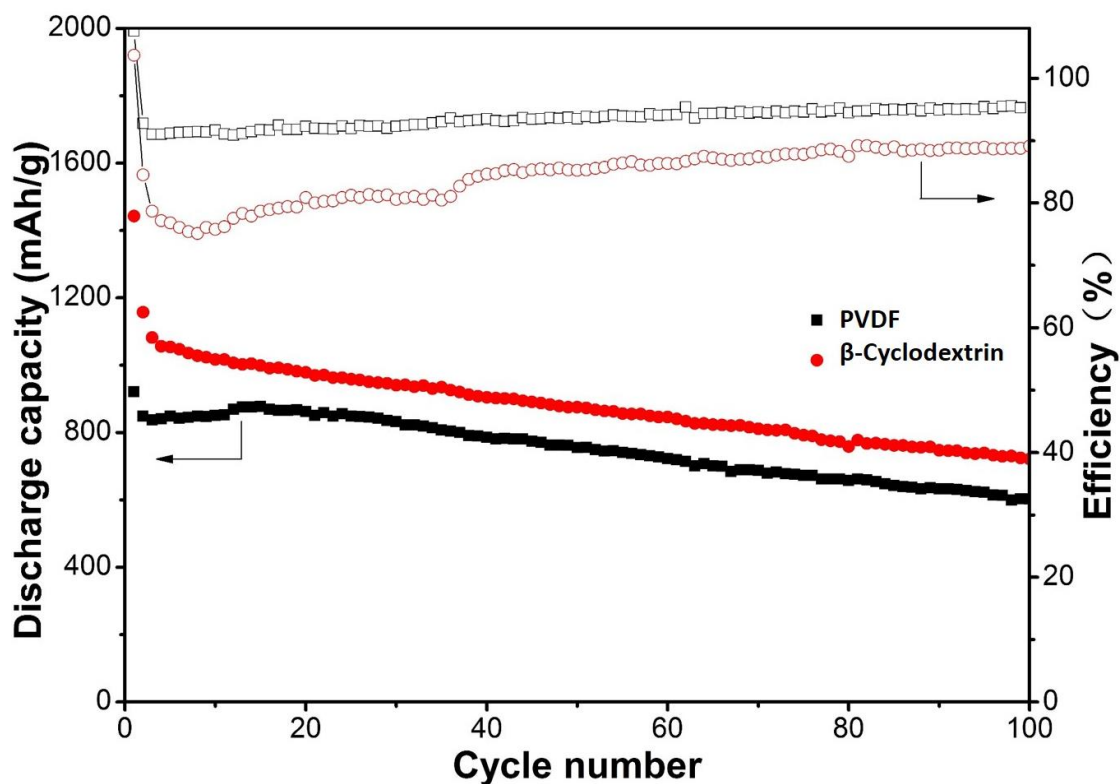


Figure 7. Cycle performance and coulomb efficiency of PS- hollow carbon /S composite electrode with PVDF and β -Cyclodextrin as the binder, current density: 100 mA g^{-1} , voltage range: 1.7-3.1V

β -Cyclodextrin is a large molecule with a ring structure, with hydrophilic external cavity and hydrophobic inner cavity[32, 33]. It can provide a hydrophobic binding site like an enzyme, and is often

used to envelop certain organic molecules, inorganic ions and gas molecules. In this paper, β -Cyclodextrin is used as a binder, and β -Cyclodextrin can significantly improve the electrochemical activity of the sulfur electrode. Fig.7 shows the circulation performance and coulomb efficiency of PS-hollow carbon /S composite electrode when PVDF and β -Cyclodextrin are used as the binder respectively. Compared with PVDF, the composite sulfur electrode with β -Cyclodextrin as binder has an average discharge capacity of about 130 mAh g⁻¹ higher per cycle, and the first cycle discharge specific capacity reaches 1445 mAh g⁻¹. It remains above 750 mAh g⁻¹ after 100 cycles. It is expected that β -Cyclodextrin can form a cladding layer on the surface of hollow carbon as well as in its pores. The polysulfide ions are bound to the interior of hollow carbon by enveloping effect, so as to further inhibit the "shuttle effect".

Table 1. Comparison of electrochemical performance of hollow carbon sphere/S electrodes

Cathode	Sulfur loading (wt%)	Initial discharge capacity(mAhg ⁻¹)	Stable discharge capacity after 100 cycles(mAhg ⁻¹)	Rate (mA g ⁻¹)	Reference
Hollow carbon sphere/S(Prepared by PAPC)	76.7%	1108	558	168	[18]
Hollow carbon sphere/S(Prepared by PS template)	74.8%	1445	750	100	This work

Table 1 compared the performance of obtained hollow carbon sphere/S composites prepared by PS template with hollow carbon sphere/S composites prepared by PAPC hollow nanospheres reported in the literature [18]. Hollow carbon sphere/S composites prepared in this paper shows outstanding performance in terms of initial discharge specific capacity, cyclic stability and capacity retention rate.

The discharge rate performance of the composite sulfur electrode with β -Cyclodextrin as the binder are shown in Fig. 8. The discharge specific capacity of the composite sulfur electrode decreases as the current density increases, but the amplitude is small. When charging and discharging current density is at 100 mA g⁻¹, 200 mA g⁻¹ and 300 mA g⁻¹, the reversible discharge capacity is 1293 mAh g⁻¹, 926 mAh g⁻¹ and 856 mAh g⁻¹, respectively, and all showed good cyclic stability. When the current density increase to 500 mA g⁻¹, the reversible discharge capacity of the electrode remains around 795 mAh g⁻¹, representing 61% of the low current density (100 mA g⁻¹). The results show that the PS- hollow carbon /S composite has good multiplying performance. However, the rate performances of HCNs-S in the literature[18], which the reversible discharge capacity is 1350 mAh g⁻¹, 718 mAh g⁻¹, 566 mAh g⁻¹ at the discharge rate of 0.1C, 0.2C and 0.5C respectively. It was found that the discharge capacity of PS-hollow carbon /S composite was 210 mAh g⁻¹ higher than the HCNs-S composite at a similar current density.

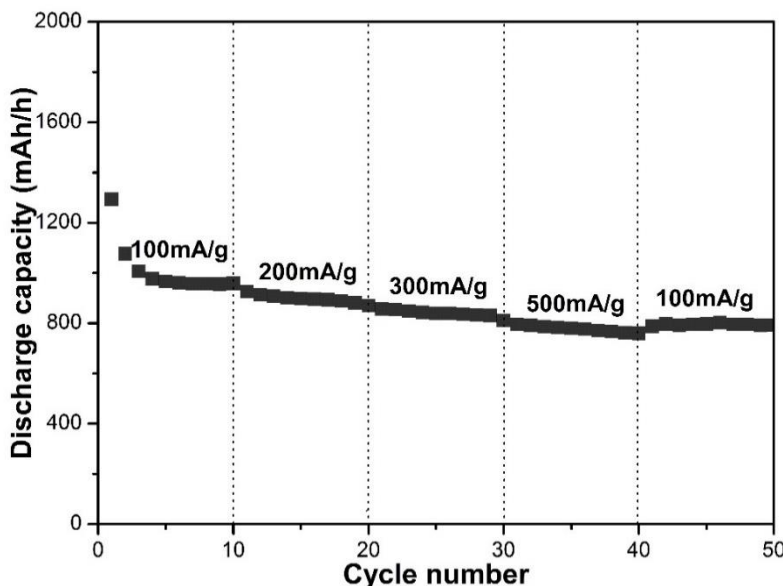


Figure 8. The discharge rate performance of PS- hollow carbon /S composite electrode, and the voltage range: 1.7v - 3.1v

4. CONCLUSION

In this paper, a high-porosity mesoporous carbon with hollow sphere structure is prepared by using PS microspheres as the template and phenolic resin as the carbon source, combining with subsequent CO₂ activation. The results show that the discharge specific capacity is 920 mAh g⁻¹ in the first cycle, and the discharge capacity remains above 600 mAh g⁻¹ after 100 cycles, with a capacity retention rate of 64.3%. The discharge specific capacity increased to 1445 mAh g⁻¹ in the first cycle after the improvement of β-Cyclodextrin as the binder, and remained above 750 mAh g⁻¹ after 100 cycles. As a sulfur electrode carrier, PS-hollow carbon porous carbon not only improves the sulfur loading of the sulfur electrode, but also has a remarkable effect in suppressing the loss of polysulfide dissolution and improving the cycle stability. In addition, β-Cyclodextrin as sulfur electrode binder can significantly improve the electrochemical activity of sulfur electrode.

ACKNOWLEDGEMENTS

This work was supported by the National Natural Science Foundation of China [grant number 21603093], Project of State Grid Jiangxi Electric Power Co., LTD. [52182018000S], the Foundation of Jiangxi Education Department [grant number GJJ161121], the National Natural Science Foundation of China [grant number 51567018], and the Foundation of Jiangxi Education Department [grant number GJJ151132].

References

1. P. Patel, *ACS Cent. Sci.*, 1 (2015) 161.
2. J.M. Tarascon, M. Armand, *Nature*, 414(2001) 359.

3. P.G. Bruce, S.A. Freunberger, L.J. Hardwick, *Nat. Mater.*, 11 (2012) 19.
4. A. Manthiram, Y.Fu, S.H. Chung, C. Zu, Y.S. Su, *Chem. Rev.*, 114 (2014) 11751.
5. J. Conder, C. Vilevieille, *Curr. Opin. Electrochem.*, 9 (2018) 33.
6. Z.W. Seh, Y. Sun, Q. Zhang, Y. Cui, *Chem. Soc. Rev.*, 45 (2016) 5605.
7. Q. Li, Z. Zhang, Z. Guo, K. Zhang, Y. Lai, J. Li, *J. Power Sources*, 274(2015) 338.
8. L. Sun, M.Li, Y. Jiang, W. Kong, K. Jiang, J. Wang, S. Fan, *Nano Lett.*, 14 (2014) 4044.
9. L. Ji, M. Rao, S. Aloni, L. Wang, E.J. Cairns, Y. Zhang, *Energy Environ. Sci.*, 4 (2011) 5053.
10. Y.B. Yang, H. Xu, S.X. Wang, Y.F. Deng, X.Y. Qin, *Electrochim. Acta*, 297 (2019) 641.
11. Z.S. Cao, C.Q. Wang, C. Jun, *Mater. Lett.*, 225 (2018) 157.
12. B. Zhang, X. Qin, G.R. Li, X.P. Gao, *Energy Environ. Sci.*, 3 (2010) 1531.
13. W.H. Zhang, D. Qiao, J.X. Pan, Y.L. Cao, H.X. Yang, X.P. Ai, *Electrochim. Acta*, 87 (2013) 497.
14. X.L. Ji, K.T. Lee, L.F. Nazar, *Nat. Mater.*, 8 (2009) 500.
15. J. Song, T. Xu, M.L. Gordin, P. Zhu, D. Lv, Y.B. Jiang, Y. Chen, Y. Yuan, D. Wang, *Adv. Funct. Mater.*, 24 (2014) 1243.
16. N. Jayaprakash, J. Shen, S.S. Moganty, *Angew. Chem. Int. Ed.*, 123 (2011) 602.
17. T. Dhawa, S. Chattopadhyay, G. De, S. Mahanty, *Mater. Chem. Phys.*, 225 (2019) 309.
18. S.Z. Zeng, Y.C. Yao, X.R. Zeng, Q.J. He, X.F. Zheng, S.S. Chen, W.X. Tu, J.Z. Zou, *J. Power Sources*, 357 (2017) 11.
19. Z. Wang, S. Zhang, L. Zhang, R. Lin, X. Wu, H. Fang, Y. Ren, *J. Power Sources*, 248 (2014) 337.
20. M.S. Park, J.S. Yu, K.J. Kim, G. Jeong, J.H. Kim, T. Yim, Y.N. Jo, U. Hwang, S. Kang, T. Woo, H. Kim, Y.J. Kim, *RSC Adv.*, 3 (2013) 11774.
21. Y. Qiu, W. Li, W. Zhao, G. Li, Y. Hou, M. Liu, L. Zhou, F. Ye, H. Li, Z. Wei, S. Yang, W. Duan, Y. Ye, J. Guo, Y. Zhang, *Nano Lett.*, 14 (2014) 4821.
22. X.D. Hong, J. Liang, X.N. Tang, H.C. Yang, F. Li, *Chem. Eng. Sci.*, 194 (2019) 148.
23. S.X. Jia, X.P. Chen, F. Ping, Z.P. Zhao, F. Chen, M.Q. Zhong, *Int. J. Electrochem. Sci.*, 13 (2018) 3407.
24. J. Ye, F. He, J. Nie, Y.L. Cao, H.X. Yang, X.P. Ai, *J. Mater. Chem. A*, 3 (2015), 7406.
25. Z. Li, L.X. Yuan, Z.Q. Yi, Y.M. Sun, Y. Liu, Y. Jiang, Y. Shen, *Adv. Energy Mater.* 4 (2014) 1301473.
26. Y. Xin, Z.L. Zhang, Y.H. Huang, D.S. Jung, T.H. Hwang, J. H. Lee, *Nano Lett.*, 14 (2014) 4418.
27. S.E. Cheon, S.S. Choi, J.S. Han, Y.S. Choi, B.H. Jung, H.S. Lim, *J. Electrochem. Soc.*, 151 (2004) A2067.
28. X.Y. Dai, X. Zhang, Y.F. Meng, P.K. Shen, *New carbon Mat.*, 26 (2011) 389.
29. R.P. Buck, E. Lindner, *Pure & Appl. Chem.* 66 (1994) 2527.
30. G. Wang, J. Yang, J. Park, X. Gou, B. Wang, H. Liu, J. Yao, *J. Phys. Chem. C*, 112 (2008) 8192.
31. P. Strubel, S. Thieme, T. Biemelt, *Adv. Mater.*, 25 (2015) 287.
32. N. Wang, Y.N. Nu Li, S.J. Su, J. Yang, J.L. Wang, *J. Power Sources*, 341 (2017) 219.
33. J. Liu, Q. Zhang, Y.K. Sun, *J. Power Sources*, 396 (2018) 19.